Supplementary Information for Urban spatial structures from human flow by Hodge-Kodaira decomposition

Takaaki Aoki,* Shota Fujishima, Naoya Fujiwara

*E-mail: takaaki.aoki.work@gmail.com.

Contents

1 Ranking of potential in the Tokyo metropolitan area from 1988 to 2018 1
2 Percentage of gradient components in London and Tokyo. 3
3 Distance deterrence effect. 3

1 Ranking of potential in the Tokyo metropolitan area from 1988 to 2018

Table S1 shows the top 20 zones by negative potential $-V$, using the commuter datasets of successive person-trip surveys from 1988 to 2018 in the Tokyo metropolitan area.

Over 30 years, *Chiyoda* city — the Imperial Palace and its surrounding areas — has been at the top of the potential. Its neighbouring cities, such as *Minato*, *Chuo*, *Shinjuku*, and *Shibuya*, had occupied the top five ranks by the potential over the years.

Some zones, such as *Naka* ward in *Yokohama* city, *Kawasaki* ward in *Kawasaki* city, and *Sumida* city, have declined in the ranking from 1988 to 2018. On the other hand, some zones, such as *Tachikawa* and *Akishima* cities and *Omiya* ward in *Saitama* city, have raised their rankings.

2018 Zone	$-V$	2008 Zone	$-V$	1998 Zone	$-V$	1988 Zone	$-V$
Chioda City	6554	Chioda City	7170	Chioda City	5916	Chioda City	6808
Minato City	5367	Minato City	6580	Minato City	4952	Chuo City	5251
Chuo City	3337	Chuo City	4454	Chuo City	4412	Minato City	5164
Shinjuku City	2927	Shinjuku City	3088	Shinjuku City	2999	Shinjuku City	2854
Shibuya City	2237	Shibuya City	2280	Shibuya City	2101	Shibuya City	1696
Shinagawa City	1358	Shinagawa City	1317	Taito City	1142	Taito City	1236
Koto City	1221	Koto City	992	Shinagawa City	1054	Naka Ward, Yokohama City	849
Bunkyo City	695	Taito City	878	Toshima City	875	Shinagawa City	665
Taito City	616	Bunkyo City	824	Naka Ward, Yokohama City	793	Toshima City	647
Nishi Ward, Yokohama City	578	Naka Ward, Yokohama City	704	Bunkyo City	783	Kawasaki Ward, Kawasaki City	633
Naka Ward, Yokohama City	513	Toshima City	682	Koto City	658	Bunkyo City	625
Atsugi City with Aikawa and Kiyokawa Areas	327	Nishi Ward, Yokohama City	561	Nishi Ward, Yokohama City	610	Nishi Ward, Yokohama City	402
Chuo Ward, Chiba City	286	Chuo Ward, Chiba City	372	Kawasaki Ward, Kawasaki City	605	Sumida City	322
Toshima City	272	Kawasaki Ward, Kawasaki City	330	Chuo Ward, Chiba City	585	Atsugi City with Aikawa and Kiyokawa Areas	191
Mihama Ward, Chiba City	217	Atsugi City with Aikawa and Kiyokawa Areas	283	Sumida City	343	Chiba City	183
Kawasaki Ward, Kawasaki City	214	Sumida City	233	Atsugi City with Aikawa and Kiyokawa Areas	207	Koto City	129
Omiya Ward, Saitama City	180	Mihama Ward, Chiba City	137	Yokosuka City	122	Meguro City	58
Tachikawa and Akishima Cities	117	Omiya Ward, Saitama City	116	Ota City	106	Ota City	47
Sumida City	85	Tachikawa and Akishima Cities	42	Meguro City	89	Narita City with Tomisato and Sakae Towns	37
Saiwai Ward, Kawasaki City	80	Yokosuka City	39	Narita City with Tomisato and Sakae Towns	85	Yokosuka City	35

Table S1. Top 20 zones of potentials in Tokyo metropolitan area from 1998 to 2018.

2 Percentage of gradient components in London and Tokyo.

The percentage R^2 was evaluated by the transport methods in the London case (Table S2) and by year in the Tokyo case (Table S3).

Transport Method	Percentage
All	52.7
Public transport	63.7
Private car	21.5

Table S2. Percentage R^2 of gradient component of home-work trips in London.

Year	Percentage
1988	42.4
1998	41.3
2008	40.8
2018	37.4

Table S3. Percentage R^2 of gradient component of home-work trips in Tokyo metropolitan area.

3 Distance deterrence effect.

Distance is obviously an important factor of human mobility. This factor has been considered as a *distance-deterrence function* $f(d)$ in spatial interaction models, such as the gravity model. We here integrate the function into the Hodge-Kodaira decomposition.

We rewrite the optimization problem in equation (3) as

$$\begin{aligned}&\min_s \left[\sum_{\{i,j\}} [f(d_{ij})(s_j - s_i) - A_{ij}]^2\right] \\ &= \min_s \left[\sum_{\{i,j\}} |f(d_{ij})|^2 \left[(s_j - s_i) - \frac{A_{ij}}{f(d_{ij})}\right]^2\right] \\ &= \min_s \left[\sum_{\{i,j\}} w_{ij}\left[(s_j - s_i) - A^w_{ij}\right]^2\right], \end{aligned} \tag{S1}$$

where

$$\begin{aligned}A^w_{ij} &:= A_{ij}/f(d_{ij}) \\ w_{ij} &:= |f(d_{ij})|^2.\end{aligned}$$

With a weighted Euclidean inner product in the space $\mathscr{A}$, $\langle X, W\rangle = \sum_{\{i,j\}} w_{ij}X_{ij}Y_{ij}$, the problem is equivalent to an l_2-projection of A onto im(grad) and the minimal norm solution s^w is given by,

$$s^w_i = -\frac{1}{N}\sum_j^N w_{ij}A^w_{ij} = -\frac{1}{N}\sum_j^N f(d_{ij})A_{ij}. \tag{S2}$$

Figure S1 shows this distance-integrated potential s^w in the London case, with a specified form of the distance-deterrence function, $f(d) = \exp(-d_{ij}/D)$. The parameter D was 31.12 km, determined by a linear regression with the formula $A_{ij} = \text{constant} \cdot \exp(-d_{ij}/D)$, using the Euclidean distance d_{ij} between the centroids of the zones. As shown in Figure S1a, the landscape of the distance-integrated potential s^w is similar to that of potential s without distance-integration. Figure S1b shows the scattering plot between s and s^w. The points lie on a line, indicating a sublinear scaling of s^w to s. This means that in the London case, the distance-deterrence effect rescales the potential s uniformly, and does not alter the relative rankings among the places by the potential.

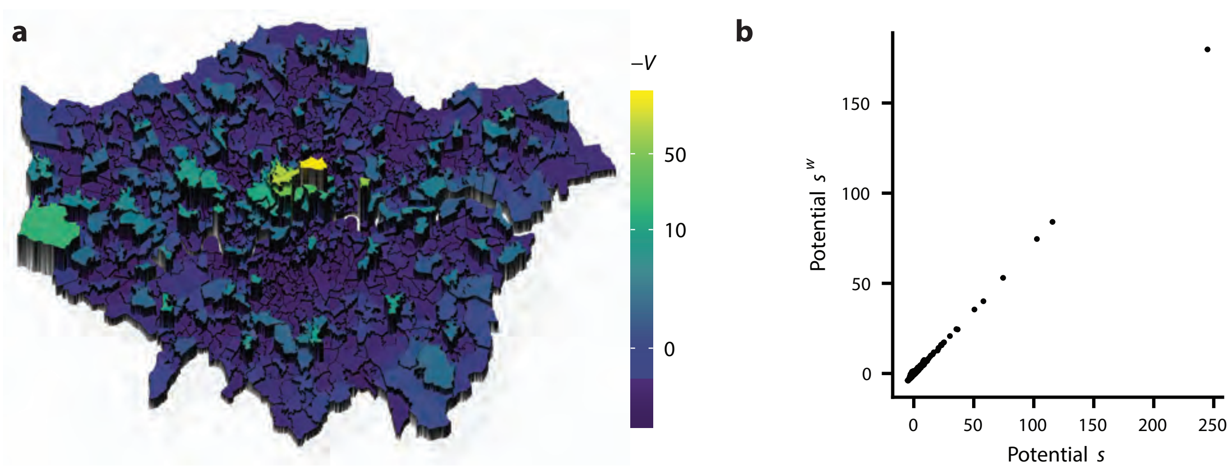

Figure S1. Distance-integrated potential s^w in the London case. (**a**) The potential is calculated by equation (S2), using the same home-work trip data in Figure 3. (**b**) Scattering plot between the potential without the distance-deterrence effect, s and with the effect, s^w.